J Physiol 588.20 (2010) pp 3901–3920

The Journal of Physiology

Connexin hemichannel-mediated CO_2-dependent release of ATP in the medulla oblongata contributes to central respiratory chemosensitivity

Robert T. R. Huckstepp[1], Rachid id Bihi[1], Robert Eason[1], K. Michael Spyer[3], Nikolai Dicke[2], Klaus Willecke[2], Nephtali Marina[3], Alexander V. Gourine[3] and Nicholas Dale[1]

[1] *Department of Biological Sciences, University of Warwick, Coventry, UK*
[2] *Institute of Genetics, University of Bonn, Bonn, Germany*
[3] *Neuroscience, Physiology and Pharmacology, University College London, London, UK*

Arterial P_{CO_2}, a major determinant of breathing, is detected by chemosensors located in the brainstem. These are important for maintaining physiological levels of P_{CO_2} in the blood and brain, yet the mechanisms by which the brain senses CO_2 remain controversial. As ATP release at the ventral surface of the brainstem has been causally linked to the adaptive changes in ventilation in response to hypercapnia, we have studied the mechanisms of CO_2-dependent ATP release in slices containing the ventral surface of the medulla oblongata. We found that CO_2-dependent ATP release occurs in the absence of extracellular acidification and correlates directly with the level of P_{CO_2}. ATP release is independent of extracellular Ca^{2+} and may occur via the opening of a gap junction hemichannel. As agents that act on connexin channels block this release, but compounds selective for pannexin-1 have no effect, we conclude that a connexin hemichannel is involved in CO_2-dependent ATP release. We have used molecular, genetic and immunocytochemical techniques to demonstrate that in the medulla oblongata connexin 26 (Cx26) is preferentially expressed near the ventral surface. The leptomeninges, subpial astrocytes and astrocytes ensheathing penetrating blood vessels at the ventral surface of the medulla can be loaded with dye in a CO_2-dependent manner, suggesting that gating of a hemichannel is involved in ATP release. This distribution of CO_2-dependent dye loading closely mirrors that of Cx26 expression and colocalizes to glial fibrillary acidic protein (GFAP)-positive cells. *In vivo*, blockers with selectivity for Cx26 reduce hypercapnia-evoked ATP release and the consequent adaptive enhancement of breathing. We therefore propose that Cx26-mediated release of ATP in response to changes in P_{CO_2} is an important mechanism contributing to central respiratory chemosensitivity.

(Received 30 April 2010; accepted after revision 20 August 2010; first published online 24 August 2010)
Corresponding author N. Dale: Department of Biological Sciences, University of Warwick, Coventry CV4 7AL, UK. Email: n.e.dale@warwick.ac.uk

Abbreviations Cx, connexin; CBX, carbenoxolone; CBF, carboxyfluorescein; FITC, fluorescein isothiocyanate; GFAP, glial fibrillary acidic protein; MAP2, microtubule associated protein 2; NPPB, 5-nitro-2-(3-phenylpropylamino)benzoic acid; RTN, retrotrapezoid nucleus; VMS, ventral medullary surface.

Introduction

Breathing is a vital function that maintains arterial partial pressures of O_2 (P_{O_2}) and CO_2 (P_{CO_2}) within physiological limits to provide O_2 for metabolism, excrete CO_2 and regulate acid–base balance. Chemosensory reflexes regulate breathing to ensure homoeostatic control of blood gases (Loeschcke, 1982; Feldman *et al.* 2003). Under some circumstances this control can be disturbed. For example at high altitude, enhanced ventilation, necessary to compensate for lower atmospheric O_2 concentration, reduces the P_{CO_2} in the blood (hypocapnia) and hence the ventilatory drive – this can result in periodic breathing (Grocott *et al.* 2009; Wilson *et al.* 2009). During central sleep apnoea arterial P_{CO_2} rises (hypercapnia) and P_{O_2} falls (hypoxia) causing arousal and resumption of breathing. Congenital central hypoventilation syndrome (CCHS) is a disorder of central chemoreception (Shea, 1997). Most patients with CCHS can adequately regulate their blood gases while awake but when asleep, these patients lose the

DOI: 10.1113/jphysiol.2010.192088

drive to breathe and will die unless artificially ventilated (Chen & Keens, 2004).

Despite the undoubted importance of central respiratory chemoreception for homoeostatic control of blood gases, the mechanisms by which this is achieved remain unclear. Several lines of evidence suggest that changes in P_{CO_2} are detected as consequent changes in pH (Winterstein, 1949; Loeschcke, 1982; Feldman *et al.* 2003; Guyenet, 2008; Nattie & Li, 2008). There are several areas of the medulla oblongata that contain pH/CO_2 sensitive neurons, especially near the highly vascularised ventral surface of the medulla oblongata (the ventral medullary surface, VMS). For example a population of neurons sensitive to changes in pH has been described in the retrotrapezoid nucleus (RTN) (Mulkey *et al.* 2004). These neurons send neurites to the VMS (Mulkey *et al.* 2004), are glutamatergic (Stornetta *et al.* 2006) and project to the ventral respiratory column. They are strong candidates for at least one class of central pH chemosensors. However the molecular mechanisms of central respiratory chemosensitivity have not been established and a possible molecular candidate – the pH sensitive TASK-1 channel – has recently been eliminated as the transducing molecule (Mulkey *et al.* 2007; Trapp *et al.* 2008). Nevertheless several other types of pH-sensitive K^+ channels could play a role in chemosensing (Wu *et al.* 2004; Yamamoto *et al.* 2008). pH-sensitive neurons of the medullary raphé and locus coeruleus have also been proposed as candidate respiratory chemosensors (Filosa *et al.* 2002; Severson *et al.* 2003; Richerson, 2004; Corcoran *et al.* 2009). Note, however, that the existence of a pH-sensing chemosensory mechanism does not preclude the possibility of parallel chemosensing pathways (Ritucci *et al.* 2005; Putnam *et al.* 2005; cf. Summers *et al.* 2002).

We have shown previously that release of ATP from the areas of the VMS corresponding to the classical chemosensory areas (Loeschcke, 1982) is an important signalling step in the central chemosensory transduction of the CO_2 stimulus (Gourine *et al.* 2005*a*). The released ATP may excite respiratory neurons via both P2X and P2Y receptors on their ventrally directed dendrites that approach the VMS (Kawai *et al.* 1996; Gourine *et al.* 2003). We have now studied in detail the mechanisms of ATP release by using an *in vitro* slice of the VMS that reliably reproduces CO_2-dependent ATP release. Our new data suggest that ATP is released in response to changes in P_{CO_2} rather than extracellular pH and occurs via gap junction hemichannels, most likely connexin 26, which demonstrates appropriate expression patterns and properties (Huckstepp *et al.* 2010) to mediate this release.

Methods

All methods required to obtain tissue for *in vitro* experiments and the *in vivo* recordings were performed in accordance with the ethical standards of *The Journal of Physiology* as set out by Drummond (2009).

In vitro experiments

Young adult Sprague–Dawley rats (4–6 weeks old) were humanely killed by an overdose of isoflurane in accordance with the UK Animals (Scientific Procedures) Act 1986. The medulla was rapidly dissected free from the skull in a bath of chilled aCSF with an additional 10 mM Mg^{2+} at a temperature between 4 and 6°C. To preserve the CO_2-sensitive ATP release mechanism, it was essential to ensure that no blood found its way to the VMS, and that the pia mater remained intact and undisturbed throughout the whole procedure. The isolated medulla was glued onto a chilled metal block ventral surface upper most and, with the aid of a Microm HM650V (Walldorf, Germany) vibrating tissue slicer, a horizontal slice 400 μm thick was cut parallel to the VMS.

Following isolation, the tissue slice was left for 30 min to recover in standard artificial cerebrospinal fluid (aCSF) at 33°C under constant superfusion at a rate of approximately 6 ml min^{-1}. The following solutions were used.

Standard aCSF: 124 mM NaCl, 3 mM KCl, 1 mM $CaCl_2$, 26 mM $NaHCO_3$, 1.25 mM NaH_2PO_4, 1 mM $MgSO_4$, 10 mM D-glucose saturated with 95% O_2–5% CO_2, pH 7.5, P_{CO_2} 35 mmHg.

80 mM HCO_3^- aCSF: 70 mM NaCl, 3 mM KCl, 1 mM $CaCl_2$, 80 mM $NaHCO_3$, 1.25 mM NaH_2PO_4, 1 mM $MgSO_4$, 10 mM D-glucose, saturated with 9%, 12% or 15% CO_2 (with the balance being O_2) to give a pH of 7.65, 7.5 or 7.35 and a P_{CO_2} of 60, 70 or 90 mmHg, respectively.

50 mM HCO_3^- aCSF: 100 mM NaCl, 3 mM KCl, 1 mM $CaCl_2$, 50 mM $NaHCO_3$, 1.25 mM NaH_2PO_4, 1 mM $MgSO_4$, 10 mM D-glucose, saturated with 6%, 9% or 12% CO_2 (with the balance being O_2) to give a pH of 7.65, 7.5 or 7.35 and a P_{CO_2} of 40, 55 or 70 mmHg, respectively.

10 mM HCO_3 aCSF: 140 mM NaCl, 3 mM KCl, 1 mM $CaCl_2$, 10 mM $NaHCO_3$, 1.25 mM NaH_2PO_4, 1 mM $MgSO_4$, 10 mM D-glucose, saturated with 2% CO_2 (with the balance being O_2) to give a pH of 7.5 and a P_{CO_2} of 20 mmHg.

All chemicals and compounds were from Sigma, unless otherwise indicated. Glycerol (2 mM) was added to all solutions to enable operation of the ATP biosensor.

ATP biosensing

ATP and null biosensors (Llaudet *et al.* 2005) were obtained from Sarissa Biomedical Ltd (Coventry, UK). These biosensors have a permselectivity layer that greatly enhances their selectivity for ATP *versus* non-specific electroactive interferents (Fig. 1*A*). They were used in conjunction with a Duostat ME200+ (Sycopel International Ltd, Jarrow, UK). The biosensors were bent so that the sensing portion (0.5 mm in length) could be laid

flat against the surface of the slice (inset Fig. 1*B*). Dual simultaneous recordings were made with the ATP and null biosensors. The null biosensors lack the ATP-sensing enzymes and act as a control for any non-specific signals (Gourine *et al.* 2005*a*,*b*; Llaudet *et al.* 2005; Pearson *et al.* 2005; Gourine *et al.* 2008). For every experiment the sensors were calibrated at the end of each recording, and tested against a potential interferent (5-HT) to assess selectivity and tested against aCSF with high P_{CO_2} to test whether this treatment affected the null and ATP biosensors equally (Fig. 1*A*). All records are presented as the differential signal between the ATP and null biosensors (Fig. 1*B*). This removes any contamination of the specific ATP signal by non-specific signals (Fig. 1*A*). The blockers used in this study did not alter the biosensors' responsiveness to ATP (Supplementary Fig. 1). Simultaneous pH measurements were made within the recording chamber by means of a miniature pH electrode (Harvard Apparatus, Edenbridge, Kent, UK).

Application of pharmacological agents

After the initial recovery period, a 5 min test stimulus of 80 mM HCO_3^- aCSF saturated with 9% CO_2 (P_{CO_2} 60 mmHg) was given followed by a 30 min wash in standard aCSF. The pharmacological agent (acetazolamide 500 μM, carbenoxolone 10 μM, carbenoxolone 100 μM, Co^{2+} 500 μM, 5-nitro-2-(3-phenylpropylamino)benzoic acid (NPPB) 200 μM, proadifen 200 μM, probenecid 1 mM, or SQ22536 (Tocris) 100 μM) was then applied for 20 min in standard aCSF to allow it to take effect. A second hypercapnic stimulus in the presence of the appropriate drug was then given. After 30 min in standard aCSF containing the drug, the tissue was washed for a further 20 min in standard aCSF before the sensors were removed (to allow measurement of the basal levels of ATP release – the tone) and the sensors calibrated.

Removal of extracellular Ca^{2+}

An initial test stimulus of 80 mM HCO_3^- aCSF saturated with 9% CO_2 was given, followed by 30 min of wash. To test the dependence of ATP release on extracellular Ca^{2+}, Ca^{2+}-free aCSF (standard aCSF in which $CaCl_2$ was replaced with $MgCl_2$ with the addition of 1 mM EGTA) was then applied for 20 min before a second application of a Ca^{2+}-free 80 mM HCO_3^- aCSF saturated with 9% CO_2 (80 mM HCO_3^- aCSF in which $CaCl_2$ was replaced with $MgCl_2$ with addition of 1 mM EGTA). This was followed by 30 min in Ca^{2+}-free aCSF. The tissue was then washed for a further 20 min in standard aCSF before the sensors were removed from the VMS (to allow measurement of the tone) and then calibrated.

Connexin blockers and zero Ca^{2+} evoked ATP release

Ca^{2+}-free aCSF was applied for 10 min. The solution was switched to Ca^{2+}-free aCSF containing a connexin

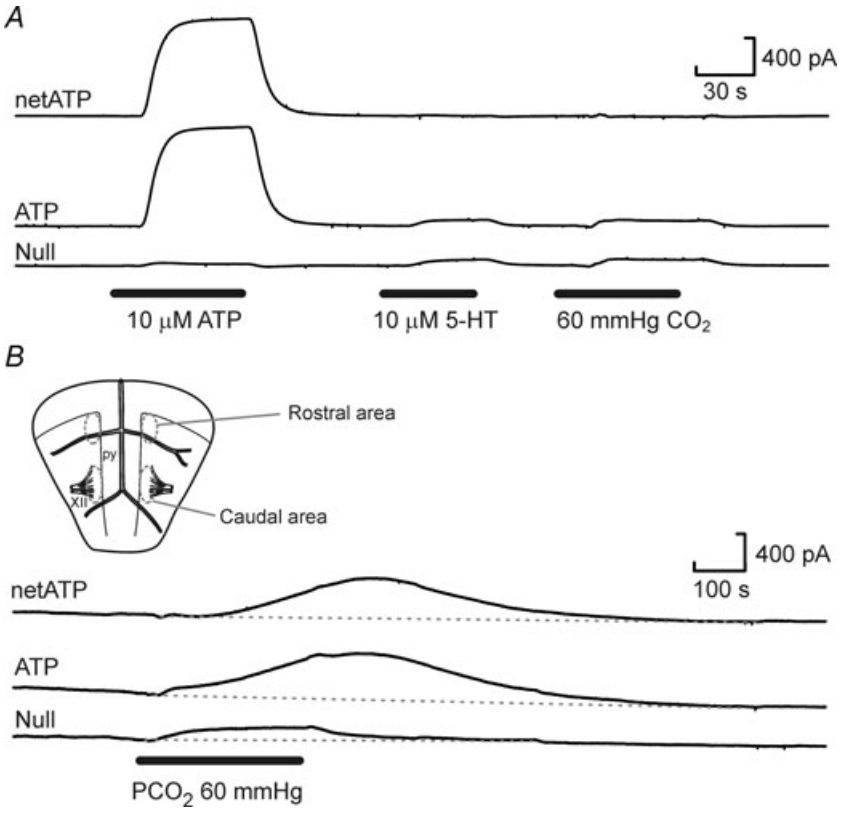

Figure 1. Selectivity, calibration and placement of biosensors
A, responses of ATP and null biosensors to ATP, 5-hydroxytryptamine (5-HT, a representative highly electroactive interferent) and the CO_2 stimulus. The small responses to 5-HT and CO_2 are very similar in the ATP and null biosensors and subtraction of the null sensor current from the ATP biosensor current gives the net ATP signal (netATP). *B*, inset shows the locations of the rostral and caudal recording areas relative to landmarks such as the pyramids (py) and XIIth nerve rootlets (XII). Responses of the ATP and null biosensors to the hypercapnic stimulus when placed at the caudal location on the ventral medullary surface.

hemichannel blocker (carbenoxolone 100 μM, Co^{2+} 500 μM, NPPB 200 μM or Proadifen 200 μM), followed by a 30 min wash in Ca^{2+}-free aCSF. The tissue was then washed for a further 20 min in standard aCSF before the sensors were removed (to allow measurement of the tone) and calibrated.

The effects of all drug applications on the magnitude of CO_2-evoked ATP release were compared to the second episode of ATP release in time-matched controls.

In vitro superfusion and timings of drug applications

Although the slice chamber (volume 1 ml) was superfused at a rapid rate, there was sufficient dead-space (volume 5 ml) in the tubing that it took around 40–50 s for the contents of the chamber to exchange following the switch of solutions. For practical reasons of accuracy, solution changes were marked on the digital recordings (and in the figures of the paper) at the time they were made rather than when the new solutions were expected to enter the chamber. This gives rise to the misleading impression of a relatively long delay in the response to changes in P_{CO_2}, which can be readily appreciated in the figures from comparing the bars marking the time at which solution changes were made with the recordings of pH, which reflects the solutions in the tissue chamber.

In vivo experiments

In vivo experiments were conducted in accordance with the UK Animals (Scientific Procedures) Act 1986. Adult male rats (260–300 g) were anaesthetised with urethane (1.6 g kg^{-1} I.P.). Adequate anaesthesia was ensured by maintaining stable levels of arterial blood pressure, heart rate and central respiratory rate and showing lack of responses to paw pinch. The femoral artery and vein were cannulated for measurement of arterial blood pressure and administration of anaesthetic, respectively. The trachea was cannulated and the animal was ventilated with a mixture of 50% oxygen and 50% nitrogen (unless otherwise required by the protocol) using a positive pressure ventilator (Harvard rodent ventilator, model 683) with a tidal volume of ~2 ml and a pump frequency similar to the resting respiratory rate (~60 strokes min^{-1}). The animal was then injected with gallamine triethiodide (Flaxedil^{TM}, 30 mg kg^{-1} I.V.; then 10 mg kg^{-1} h^{-1} I.V.) and was placed in a stereotaxic frame. The VMS was then exposed as described previously (Gourine *et al.* 2005*a*,*b*).

Activity of the phrenic nerve was recorded as an indicator of central respiratory drive. The signal was amplified (×20,000), filtered (500–1500 Hz) and rectified and smoothed ($\tau = 50$ ms). Partial pressures of O_2 and CO_2 as well as pH of the arterial blood were measured every 1–2 h. End-tidal levels of CO_2 were monitored on-line using a fast-response CO_2 analyser (model Capstar-100, CWE Inc., Ardmore, PA, USA) and kept at a designated level by altering tidal volume and respiratory frequency. In all the experiments P_{O_2} in the arterial blood was kept at >100 mmHg to ensure minimal drive from the peripheral chemoreceptors. The body temperature was maintained with a servo-controlled heating pad at 37.0 ± 0.2°C.

ATP and null sensors were each connected to a separate MicroC potentiostat (WPI, Sarasota, FL, USA) and held on a stereotaxic micromanipulator. The sensors were aligned parallel to the pyramidal tracts and then were placed in a direct contact with the VMS 0.1–0.5 mm lateral from the tracts (adjacent to, but not on top of, the major blood vessels, see Fig. 1c of Gourine *et al.* 2005*a*). The sensitive part of the sensor was ~0.5 mm in length placed over a significant portion of the VMS chemosensitive areas just rostral from the XII nerve roots (corresponding to the caudal position used with the *in vitro* slices). The identical placement of the ATP sensors and null sensors was achieved by aligning them to the pyramidal tracts, landmark blood vessels and by means of the vernier scale of the manipulator. Once the sensors were placed, the exposed area of the brain and both sensors were covered with an excessive volume of modified Bulmer's buffer (100 mM NaCl, 10 mM phosphate buffer, 1 mM $MgCl_2$ and 2 mM glycerol) and a period of 20–30 min was allowed until a steady baseline was obtained.

Quantitative PCR

A sequence of 300 μm horizontal slices (cf. Fig. 1) were cut along the ventral–dorsal axis of medullas isolated from 5- to 6-week-old rats. The RNA of each slice was extracted using the RNeasy kit (Qiagen, Valencia, CA, USA). Reverse transcription (by standard methods) was performed and the resultant cDNA was used in subsequent quantitative PCR (QPCR) analysis using an Applied Biosystems (Foster City, CA, USA) Real Time 7000. Rat β-actin, connexin 26, 32, 36 and 43, and pannexin 2 primers were designed using the primer design package (Primer Express) supplied with the Applied Biosystems Real Time 7000 and were synthesised by Invitrogen. Each QPCR reaction was performed in triplicate and the experiment was performed three independent times (3 rats).

Primer sequences were: β-actin forward AGGCCAACCGTGAAAAGATG and reverse GCCTGGATGGCTACGTACATG; Cx26 forward GGGAGAGGATGAGGCAACCT and reverse AATGTTTGCCCGGGAGATG; Cx32 forward CCAACACGGTGGACTGCTT and reverse AGGCGGCGAGCATAAAGA; Cx36 forward CCTACGGAGAAGACGGTCTTTC and reverse AGGCGGCGAGCATAAAGA; Cx43 forward TTTCCCCGACGACAACCA and reverse TGGCTAATGGCTGGAGTTCAT; and pannexin 2 forward GCTGGTCACCCTGGTCTTCA and reverse CAGTAGCCACGGGCGTACA.

$Cx26^{+/LacZ}$ knock-in mouse

This mouse strain was generated in the Institute of Genetics, University of Bonn (Germany). The mice were kept under standard housing conditions with a 12 h–12 h dark–light cycle with food and water provided *ad libitum*. Experiments were carried out in accordance with local and state regulations for research with animals in Gemany. The knock-in mouse strain was generated to study Cx26 expression by analyses of *LacZ* reporter gene expression or, alternatively, substitution of Cx26 by Cx32. In $Cx26^{+/LacZ}$ mice the coding region of Cx26 was heterozygously replaced by the lox-P-sites-flanked (floxed) *LacZ* coding region preceded by a nuclear localization signal and followed by the coding region of Cx32. Endogenous Cx26 promoter activity causes expression of Cx26 from the wild-type allele and *LacZ* reporter gene expression from the transgenic allele. Cx32 expression can only be driven under control of the endogenous Cx26 promoter ($Cx26^{+/Cx32}$ mice) after Cre mediated excision of the floxed *LacZ*-coding DNA. In this report only the floxed $Cx26^{+/LacZ}$ mice were used to study Cx26 expression in the brain by analyses of β-galactosidase activity. Enquiries about these mice should be directed to K. Willecke (Bonn).

Immunocytochemistry

Horizontal slices 400 μm thick containing the VMS from 5- to 6-week-old rats were fixed in 4% paraformaldehyde (PFA) in 0.1 M phosphate buffer pH 7.4 for 45 min at room temperature. Brains from the $Cx26^{+/lacZ}$ mice were fixed with 4% PFA in phosphate-buffered saline (PBS) via cardiac perfusion and then post-fixed in 4% PFA by the Bonn lab in accordance with local and state regulations for research with animals in Germany. Fixed tissue was placed in 30% sucrose in 0.1 M phosphate buffer, pH 7.4 and left overnight at 4°C. The fixed tissue was then embedded in Cryo-M-Bed (Bright Instruments, Huntingdon, UK) and re-sectioned into 20 or 60 μm transverse sections. All primary and secondary antibodies were made up in immunosolution (0.1 M phosphate buffer, 0.1% BSA, 0.1% sodium azide, 0.4% Triton X-100, pH 7.4). Slices were incubated overnight at 4°C in 10% normal horse serum. Chick anti-glial fibrillary acidic protein (GFAP) (Chemicon, Temecula, CA, USA) and mouse anti-Cx26 (Invitrogen) were applied at 1:500 and 1:200 respectively and incubated overnight at 4°C. The slices were then washed in 0.1 M phosphate buffer and were incubated with appropriate secondary antibodies for 2 h (Alexa Fluor 488 goat anti-mouse for Cx26 and Alexa Fluor 594 goat anti-chick for GFAP (both obtained from Invitrogen). In rats, astrocytes residing in close proximity to the VMS were also identified by cell-specific green fluorescent protein (GFP) expression driven by the GFAP promoter followed by immunohistochemical detection of Cx26. In accordance with the UK Animals (Scientific Procedures) Act 1986, adult male Sprague–Dawley rats were injected intramuscularly with a mixture of ketamine (60 mg kg^{-1}) and medetomidine (250 μg kg^{-1}) and were placed in a stereotaxic frame. Animals received two bilateral microinjections (1 μl each, stereotaxic coordinates from Bregma, AP: −10.5 mm, L −2.0 mm, V −8.5 mm) into the rostral ventrolateral medulla of an adenoviral vector to express GFP under the control of the enhanced astrocyte-specific GFAP promoter (generously provided by Prof. S. Kasparov, University of Bristol). The rats were intracardially perfused 10 days after the injections, the brainstem was isolated, and sliced and coronal sections (30 μm) were immunostained for Cx26 as described above.

Some sections (in this case 60 μm thick) were processed as free-floating sections. In these instances sections were also stained for microtubule associated protein 2 (MAP2; 1:500, Sigma) and β-galactosidase (1:1000, Sigma) with appropriate secondary antibodies. Slices were finally mounted in Vectashield DAPI (Vector Laboratories, Inc., Burlingame, CA, USA) and examined with an SP2 Leica confocal microscope.

Dye loading

Medullary slice. After preparing the slice as above and an initial 20 min recovery period, 80 mM HCO_3^- aCSF saturated with 9% CO_2 containing either carboxyfluorescein (CBF, 100 μM) or fluorescein isothiocyanate (FITC, 100 μM) was applied for 5 min, followed by a wash of 30 min in standard aCSF. Controls underwent a 5 min application of the fluorescent compound in standard aCSF followed by a 30 min wash. To wash out the dye previously loaded into the tissue, a 5 min application of 80 mM HCO_3^- aCSF saturated with 9% CO_2 was given in the absence of the dye, followed by a 10 min wash in standard aCSF. These experiments were performed on the ventral medullary slice from three rats – each replicate gave the same result.

Statistical analysis

Statistical comparisons were made by one-way ANOVA, the Kruskal–Wallis test (for data with higher variance) or Student's paired sample *t* test where appropriate. Values quoted in the text are means ± S.E.M.

Results

In vitro recapitulation of CO_2-evoked ATP release from the VMS

We first used *in vitro* preparations (horizontal slices of the medulla oblongata) to examine in detail the mechanisms

of CO_2-evoked ATP release from the VMS chemosensitive areas.

Hypercapnic acidosis (an increase in P_{CO_2} at constant [HCO_3^-] resulting in a decrease of extracellular pH to 7.1) can evoke ATP release but this was rarely repeatable more than once in a single preparation (Supplementary Fig. 2, cf. Gourine *et al.* 2005*a*). During moderate hypercapnia *in vivo*, the extracellular pH at the ventral surface of the medulla oblongata usually decreases by 0.1–0.2 units of pH (Loeschcke, 1982; Eldridge *et al.* 1985). We have consequently explored the dependence of ATP release on changes in P_{CO_2} and pH by also altering bicarbonate levels during the CO_2 stimulus.

An increase in P_{CO_2} in aCSF containing 80 mM HCO_3^- saturated with 9% CO_2–91% O_2 (P_{CO_2} 60 mmHg, pH 7.65) reliably evoked ATP release in the caudal chemosensitive area of the VMS (just medial to the emergence of the rootlets of the XIIth nerve Fig. 2*A*, *B* and *E*). ATP was also released in response to CO_2 from the dorsal side of the 400 μm thick ventral slice (Fig. 2*C* and *E*); but not from the ventral side of the second slice of the medulla cut in the ventral to dorsal progression (Fig. 2*C* and *E*). We also observed CO_2-dependent ATP release from the rostral chemosensitive area (immediately ventral to the RTN, Fig. 2*D* and *E*). Outside of the rostral and caudal VMS areas, e.g. at more lateral locations, very little CO_2-evoked ATP release was detected (Fig. 2*F*). The rostral and caudal release areas for ATP release correspond to those described in our earlier localization of sites of CO_2-evoked ATP release at the VMS *in vivo* (Gourine *et al.* 2005*a*) and respectively lie ventral to the RTN and the serotonergic neurons of the medullary raphé (Bradley *et al.* 2002).

Interestingly, we detected a high basal concentration (tone) of ATP of $3.2 \pm 0.9\,\mu$M ($n = 13$) at the VMS (Fig. 2*G*). It was absent from the ventral side of the second more dorsal slice ($0.1 \pm 0.3\,\mu$M, $n = 4$, Fig. 2*G*), suggesting that this tone is a hallmark of the ventral medullary chemosensitive areas. To our knowledge, this is an unprecedented high basal level of extracellular ATP, as in most areas of the brain ATP is rapidly broken down to adenosine and other downstream purines. That this tone exists, suggests both a significant continuous rate of basal release and a slower rate of hydrolysis of extracellular ATP in the medullary areas near the VMS compared to other brain regions.

ATP release depends on P_{CO_2}

We next examined the dependence of ATP release from the VMS on extracellular pH and P_{CO_2} by systematically changing P_{CO_2}, pH and [HCO_3^-] in the milieu (Fig. 3). We found that at a given extracellular pH, ATP release depended on the level of P_{CO_2}. Increasing P_{CO_2} to 55 mmHg and further to 70 mmHg (at constant extracellular pH) evoked release of progressively larger concentrations of ATP (Fig. 4*A*). Thus, CO_2-dependent ATP release does not require extracellular acidification, but instead depends upon prevailing levels of P_{CO_2} (Fig. 4*C*). At a constant pH of 7.5, when P_{CO_2} was reduced to 20 mmHg (from the control level of 35 mmHg) a loss of the ATP tone was seen (Fig. 4*A*). This is significant as it suggests that bidirectional changes in ATP can signal both decreases and increases in P_{CO_2}.

The systematic experimental variation of pH and P_{CO_2} also revealed that pH alters the set point of the relationship between CO_2 and ATP release from the VMS (Fig. 4*B*). At alkaline pH smaller absolute levels of P_{CO_2} were required to achieve the same concentrations of ATP release in comparison to that at lower levels of pH.

We next studied the possible mechanisms by which CO_2 could evoke release of ATP. In principle this release could be triggered by changes in extracellular pH, intracellular pH, [HCO_3^-] or P_{CO_2} itself. Our data (Figs 3 and 4) exclude a decrease in extracellular pH as a stimulus for ATP release. Changes in intracellular pH, which follow changes in P_{CO_2}, could potentially induce ATP release. Applications of NH_4Cl (20 mM, $n = 5$) to alter intracellular pH did not cause a statistically significant change in the extracellular level of ATP at the VMS (mean change $-0.3 \pm 0.3\,\mu$M); however in 3 of these 5 cases this treatment caused a loss of extracellular ATP (Fig. 5*A*). Addition of 5 mM propionate did not cause any release of ATP ($n = 3$, data not shown). CO_2 could conceivably trigger release via an increase in intracellular [HCO_3^-]. We therefore used acetazolamide to inhibit the enzyme carbonic anhydrase (cf. Nattie & Li, 1996), which catalyses the reaction of CO_2 with water. Acetazolamide by itself did not induce ATP release. However, by reducing the rate of formation of HCO_3^-, it should delay and reduce CO_2-evoked ATP release, if this were to depend on either HCO_3^- or intracellular pH. However it had no effect (Fig. 5*B* and *D*), suggesting that changes in intracellular [HCO_3^-] or pH are not the proximal stimulus for ATP release. Although there is evidence for a CO_2/HCO_3^--sensitive adenylate cyclase (Mittag *et al.* 1993; Raven, 2006), SQ22536, a blocker of adenylate cyclase, had no effect on the amplitude of CO_2-evoked ATP release (Fig. 5*C* and *D*). Furthermore we analysed the integral of CO_2-triggered ATP release in the presence of SQ22536 (area under the curve) and found that it was 764 ± 238 mM s ($n = 7$) compared to a control value of 551 ± 98 mM s ($n = 16$). This eliminates the potential contribution of a cAMP-dependent signalling pathway to CO_2-dependent ATP release.

CO_2-evoked ATP release does not require extracellular Ca^{2+} and is gap junction hemichannel dependent

We next tested the Ca^{2+} dependence of CO_2-evoked ATP release. Application of aCSF lacking Ca^{2+} (with 2 mM Mg^{2+} to maintain the total divalent ion concentration

and 1 mM EGTA to chelate any residual Ca^{2+}) by itself induced a profound release of ATP ($4.0 \pm 0.6\ \mu$M, $n = 4$, Fig. 6*A*). However, an increase in P_{CO_2} still evoked release of ATP on top of this elevated baseline ($2.0 \pm 0.5\ \mu$M, $n = 4$, not significantly different from the concentration of ATP released under control conditions, Fig. 2*A* and *E*). CO_2-evoked ATP release is therefore independent of extracellular Ca^{2+}.

That lowered extracellular Ca^{2+} could evoke ATP release suggested gap junction hemichannels as conduits for ATP release, as all of these channels will gate open in the absence of extracellular Ca^{2+} (Muller *et al.* 2002). We found

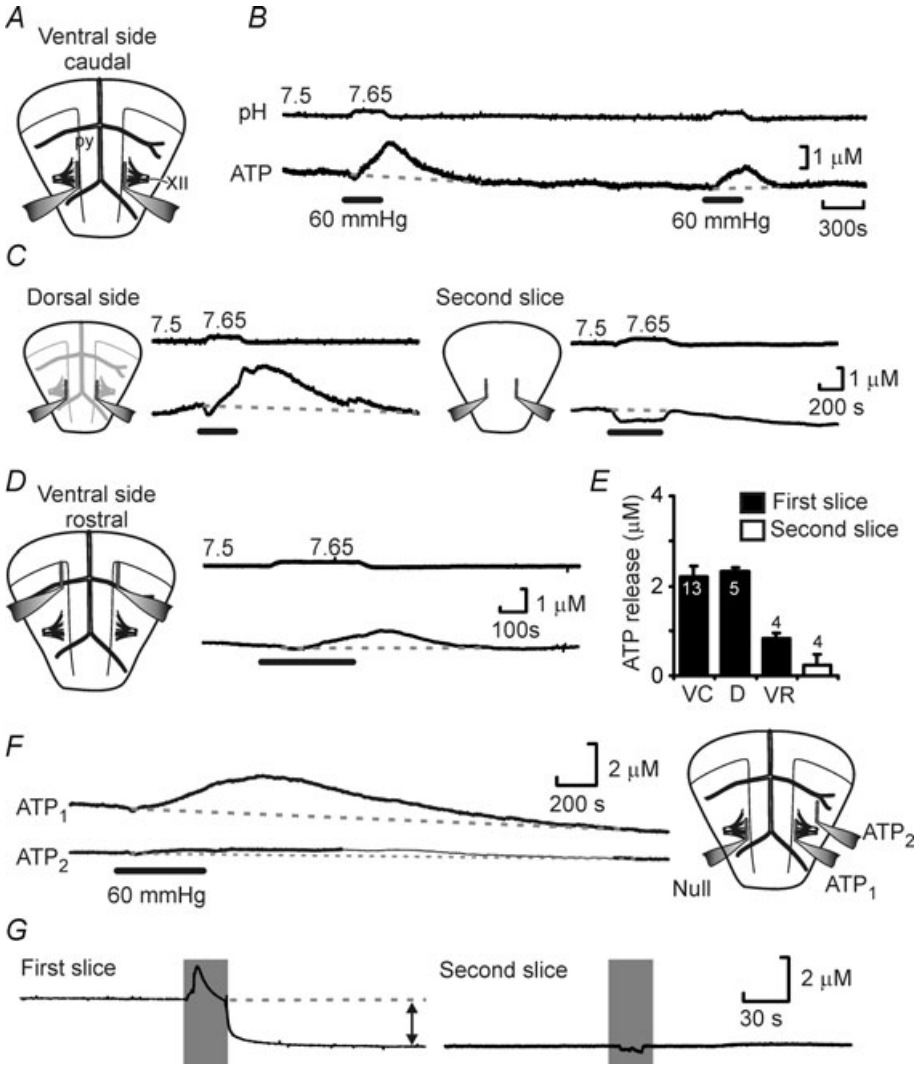

Figure 2. CO_2-evoked ATP release *in vitro*
A, diagram of the ventral surface of the ventral medullary slice showing location of the pyramids (py) and XIIth nerve rootlets (XII) and the major blood vessels along with ATP and Null biosensor placements. *B*, simultaneous recording of bath pH and net ATP release (difference in current between ATP and Null sensors) in response to a CO_2 stimulus of 60 mmHg. *C*, ATP release can be observed from the dorsal surface of the first slice (left) but not from the ventral surface of the second slice in the sequence (right). The negative shift in the sensor trace is due to pH sensitivity of the biosensor. *D*, CO_2-evoked ATP release could also be observed in a rostral position close to the RTN. *E*, summary comparing the magnitude of CO_2 evoked ATP release in the ventral slice caudal position (VC), ventral slice dorsal surface (D) and ventral slice rostral position (VR). The groups are significantly different (Kruskal–Wallis test $P = 0.001$); the release from the second slice is not significantly different from zero; all other groups are significantly different from zero. *F*, ATP release is localized on the ventral surface. Recordings from two ATP biosensors (positions shown in diagram on right) showing excellent release from the caudal position but little release from a lateral position. *G*, there is a substantial ATP tone present at the surface of the ventral slice (left) but not on surface of the second slice (right). The sensors were removed from the slice (indicated by grey shading). With the first slice there was a substantial fall of sensor signal indicative of a tone but no such change was seen with the second slice.

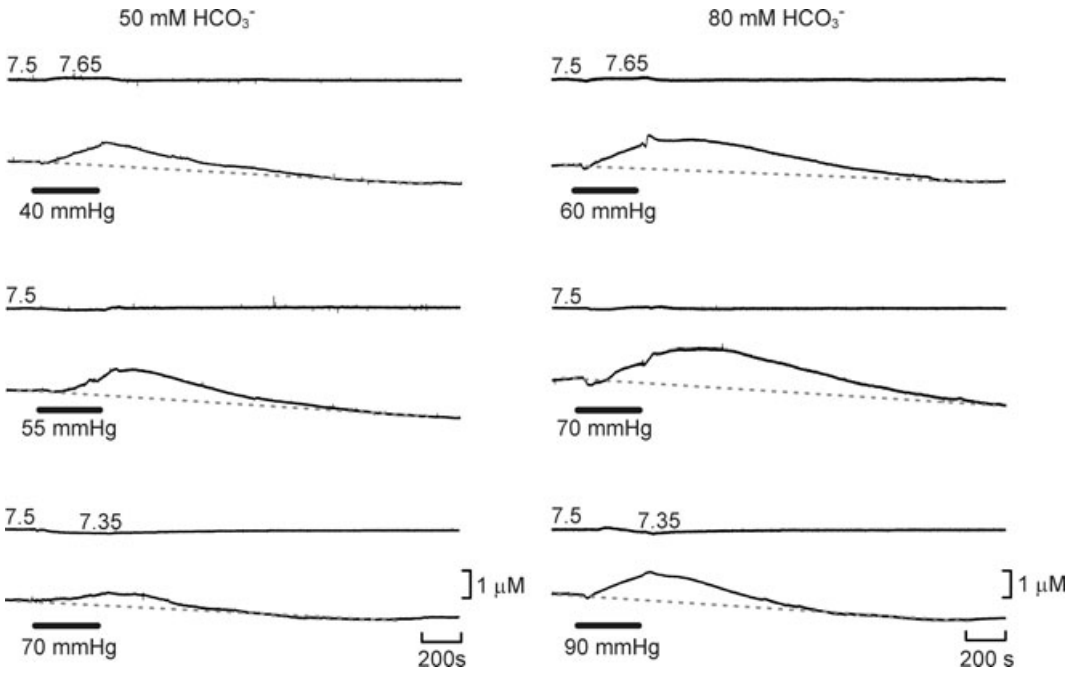

Figure 3. The dependence of ATP release on P_{CO_2}, HCO_3^- and pH
Examples of ATP release evoked by elevations in P_{CO_2} at different levels of HCO_3^-. At any given pH, higher levels of P_{CO_2} (and HCO_3^-) evoke more ATP release. Reducing extracellular pH gives less ATP release. Each recording is from a separate slice.

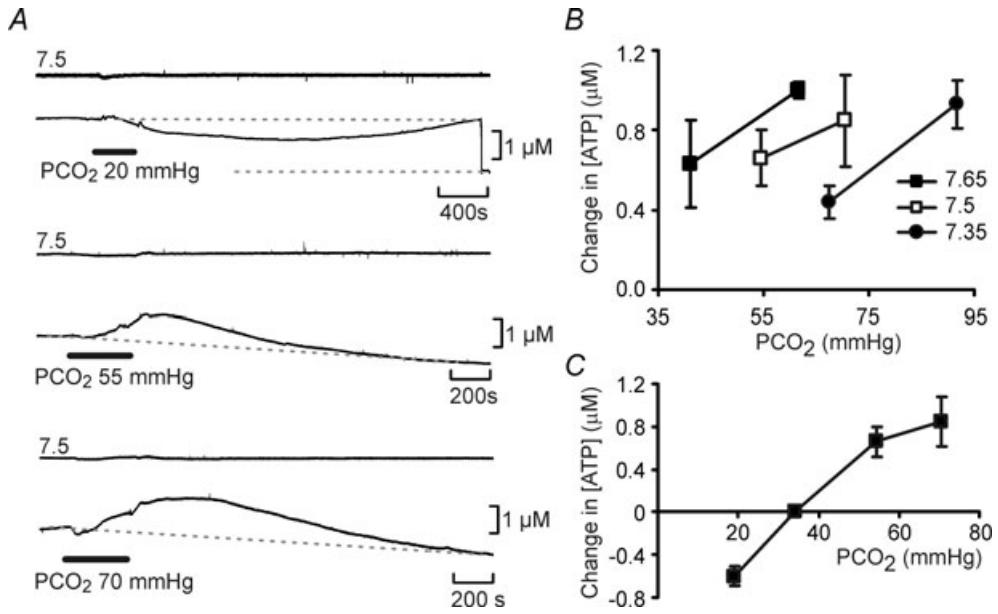

Figure 4. ATP release correlates with P_{CO_2}
A, at a constant pH (7.5), P_{CO_2} was altered from its control value (35 mmHg) to 20, 55 and 70 mmHg (bar). When P_{CO_2} was reduced there was a loss of tone (indicated by grey dashed lines – sensor removed from slice at the end of the record. Increasing P_{CO_2} resulted in progressively greater ATP release. Each recording from a different slice. *B*, summary of ATP release *versus* P_{CO_2} at three different levels of pH. Acidification decreases the sensitivity of ATP release to changes in P_{CO_2} – rightward shift of the points ($n = 4$ slices for each point). *C*, summary of evoked ATP release *versus* P_{CO_2} at pH 7.5.

that several gap junction hemichannel blockers including carbenoxolone, Co^{2+}, proadifen and NPPB all blocked the zero Ca^{2+}/EGTA induced release of ATP (Fig. 6*A* and *B*). These agents also greatly reduced the CO_2-evoked ATP release and to a lesser extent the basal tone of ATP found at the caudal area of the VMS (Figs 7*A* and *B* and 8).

Pannexin 1 forms hemichannels and has been reported to release ATP. Its action can be discriminated by application of carbenoloxolone at lower concentrations (which do not block connexin hemichannels) and by the use of probenecid (Bruzzone *et al.* 2005; Silverman *et al.* 2008). While carbenoxolone, blocked ATP release at 100 μM (see above and Fig. 7), it had no effect on CO_2-evoked ATP release at the lower dose of 10 μM (Fig. 9*A* and *B*). Similarly, CO_2-evoked ATP release was not affected by 1 mM probenecid (Fig. 9*A* and *B*). This pharmacological profile eliminates pannexin-1 as the conduit for ATP release but is consistent with a connexin hemichannel being involved.

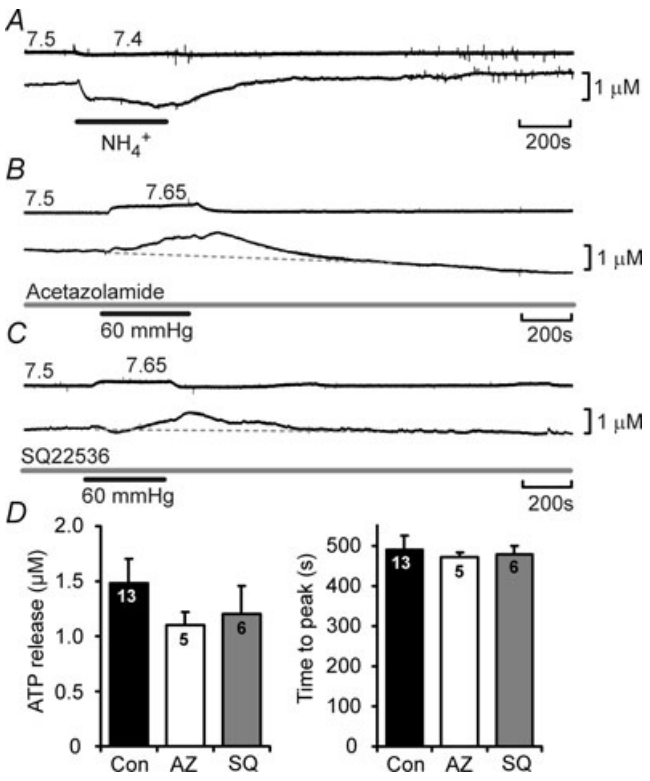

Figure 5. CO_2-evoked ATP release cannot be mimicked by changes in intracellular pH or altered by inhibition of carbonic anhydrase or adenylate cyclase
A, application of 20 mM NH_4Cl to alter intracellular pH did not cause evoked ATP release. *B*, acetazolamide, a blocker of carbonic anhydrase, at 500 μM had no effect on the magnitude or time course of CO_2-evoked ATP release. *C*, SQ22536, a blocker of adenylate cyclase, at 100 μM had no effect on the magnitude or time course of CO_2-evoked ATP release. *D*, summary bar graphs demonstrating that neither acetazolamide nor SQ22536 had an effect on the magnitude or timing of ATP release.

Expression of gap junction proteins in the medulla oblongata

There are many different types of gap junction proteins that can form functional hemichannels including connexins and pannexins. After first using conventional RT-PCR to probe the presence of connexin and pannexin mRNA in the whole medulla oblongata, we used quantitative PCR (QPCR) to determine how the expression of connexin and pannexin mRNA varied at different levels along its ventro-dorsal axis. Whilst connexins 32, 36 and 43, and pannexin 2 were roughly uniformly distributed throughout the medulla, connexin 26 (Cx26) was expressed predominantly in the first 300 μm of tissue (relative to the ventral surface, Fig. 10*A*). Whilst Cx26 demonstrated a preferential localization in the first 300 μm of tissue relative to the other tissue sections, Cx43 and Cx32 were more highly expressed in this location (6.5 ± 2.5- and 2.6 ± 0.96-fold more prevalent, respectively). By contrast Cx36 and pannexin 2 were much less abundant (0.27 ± 0.12- and 0.11 ± 0.10-fold less prevalent, respectively).

The QPCR data demonstrate the relative abundance of mRNA but do not demonstrate cellular localization. We therefore examined tissue in which a LacZ reporter had been knocked into the Cx26 locus (see Methods;

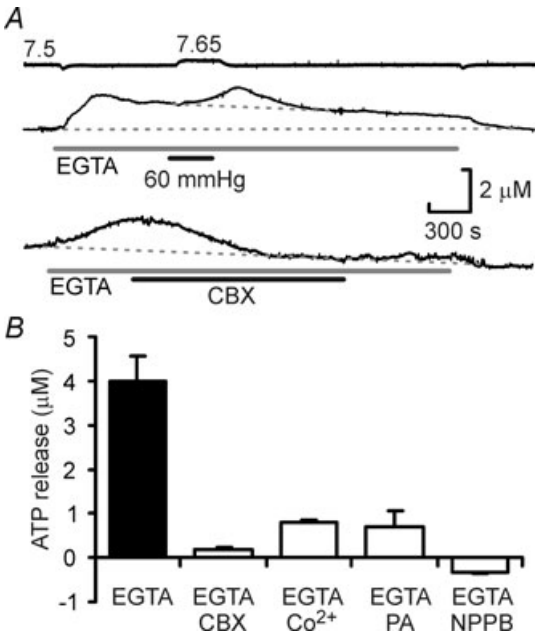

Figure 6. CO_2-dependent ATP release does not require extracellular Ca^{2+}
A, removal of extracellular Ca^{2+} (and addition of 1 mM EGTA) evokes ATP release. Top, however an increase in P_{CO_2} can still triggers further ATP release on top of this elevated baseline. Bottom, the EGTA/zero Ca^{2+} evoked ATP release can be blocked by 100 μM carbenoxolone (CBX). *B*, summary of the effect of several gap junction channel blockers on the EGTA-evoked ATP release. The blockers significantly reduce the magnitude of ATP release ($P < 0.001$, Kruskal–Wallis test).

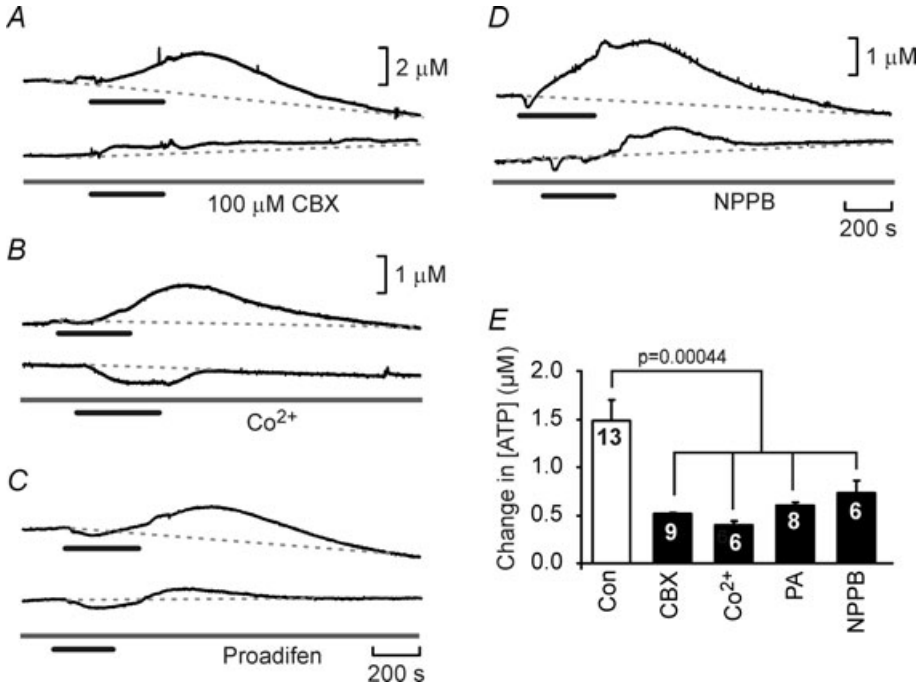

Figure 7. Gap junction hemichannel antagonists greatly reduce CO_2-evoked ATP release
A–D, recordings of CO_2-evoked ATP release before and after the application of 100 μM CBX (*A*), 500 μM Co^{2+} (*B*), 200 μM proadifen (*C*) and 200 μM NPPB (*D*). All these agents greatly reduced the release of ATP. *E*, summary statistics demonstrating the reduction of ATP release by these agents. For the comparison the second episode of ATP release was analysed in both the control (no drug) and drug treated slices to allow for the rundown of ATP release apparent in the slice preparation (see Methods). The blockers significantly reduced ATP release (ANOVA, $P = 0.00044$).

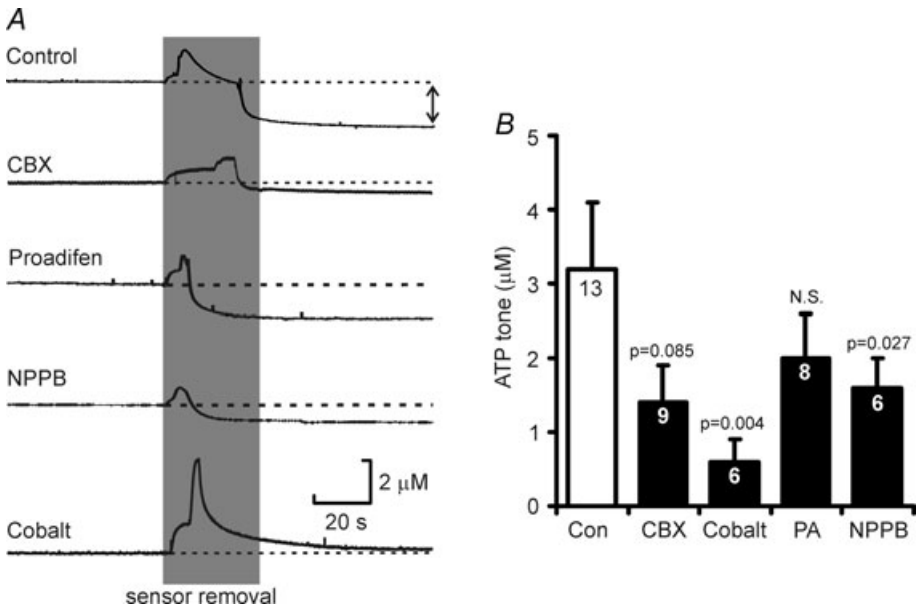

Figure 8. The basal levels of ATP at the ventral surface of the medulla can be blocked by gap junction hemichannel antagonists
A, the effect of several agents on the ATP tone recorded following removal of ATP biosensors from the surface of the slice (indicated by double headed arrow for control case). *B*, summary statistics showing the effect of these antagonists on the magnitude of the resting ATP tone. Analysis suggests that the samples are not drawn from the same population ($P = 0.029$, Kruskal–Wallis test). The probabilities next to the bars indicate pairwise comparisons to the control.

cf. Filippov *et al.* 2003). The tissue was derived from heterozygotes as deletion of the Cx26 gene is embryonic lethal. We found that in these transgenic mice *LacZ* was expressed in the leptomeninges, the glia limitans, and in nuclei near the penetrating blood vessels (Fig. 10*B–H*). This pattern of Cx26 expression was also confirmed by immunocytochemical localization of Cx26 protein in the rat medulla oblongata. As reported by others (Nagy *et al.* 2001; Mercier & Hatton, 2001; Solomon *et al.* 2001), Cx26 immunoreactivity in the ventral medulla oblongata was confined to the very ventral margin of the parenchyma, the surface of astrocytes surrounding penetrating vessels at the VMS and the pia mater (Fig. 11). Interestingly Cx26-positive puncta were also observed on many processes of astrocytes which reside at and near the VMS (Fig. 11). We note that the distribution of Cx26 that we found both by knock-in reporter expression and immunocytochemical staining was much more restricted than that reported in earlier studies (Solomon *et al.* 2001).

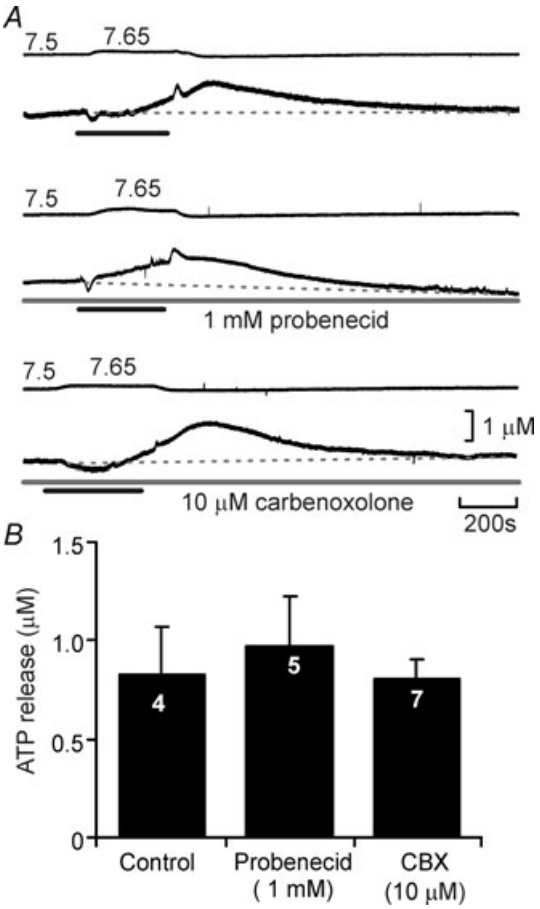

Figure 9. Pannexin-1 hemichannels are not involved in CO_2-evoked ATP release
A, neither probenecid at 1mM, nor carbenoxolone at 10 μM, both agents selective for pannexin-1 hemichannels, affected CO_2-evoked ATP release. *B*, summary bar graph demonstrating the lack of effect of probenecid and carbenoxolone on ATP release compared to interleaved controls.

Identity of VMS cells responding to changes in P_{CO_2}

Our data suggest that CO_2-dependent ATP release occurs via a hemichannel opening. Furthermore we have demonstrated that within the medulla oblongata Cx26 has a specific pattern of expression predominantly localized to

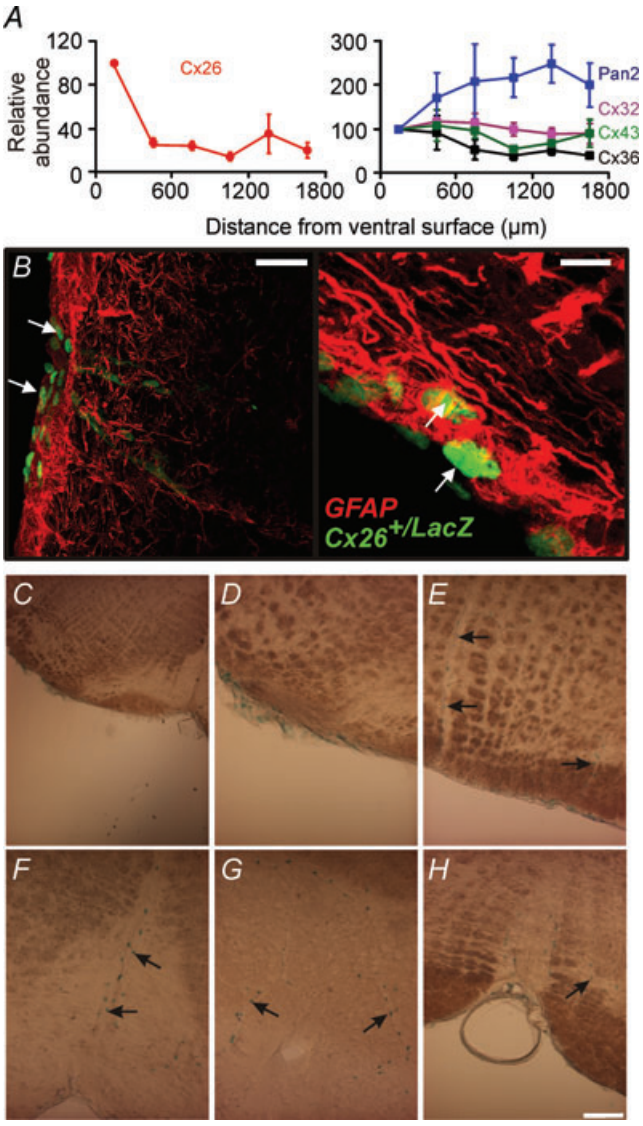

Figure 10. Localization of Cx26 in the ventral medulla oblongata
A, quantitative PCR demonstrates that mRNA for Cx26 is enriched within the first 300 μm of tissue from the ventral surface of the medulla in rat, while the mRNA of other connexins is more uniformly distributed. *B*, localization of LacZ immunoreactivity at the ventral surface of the medulla oblongata (white arrows) in mouse $Cx26^{+/LacZ}$ tissue. It is found in the leptomeninges, marginal glial cells and cells close to blood vessels. Tissue was co-stained with GFAP to label glial cells. Scale bar 40 μm (left) and 10 μm (right). *C–E*, localization of LacZ activity in the leptomeninges and along penetrating blood vessels in the ventrolateral medulla, at the same rostrocaudal level of the sites of ATP release. *F–H*, localization near the midline of the ventral medulla in the vicinity of the raphé nucleus. Black arrows indicate lacZ-positive nuclei adjacent to blood vessels (*C–H*). Scale bar 100 μm.

near the VMS. This suggests that Cx26 may mediate the ATP release in response to CO_2. If this hemichannel opens when P_{CO_2} increases to allow egress of ATP it should also allow entry of a dye (of appropriate size and charge) that would enable identification of the cells that express the hemichannel and respond to changes in P_{CO_2}.

We therefore attempted to load ventral medullary slices in a CO_2-dependent manner either with CBF for live tissue studies or FITC for subsequent fixation and counter-staining. The presence of CBF under control conditions caused some background loading (presumably through the spontaneous gating of hemichannels). This loading was greatly increased following exposure of the slice to increased levels of P_{CO_2} ($n = 3$, Fig. 12*A*). Subsequent exposure of the slice to hypercapnia in the absence of CBF reduced the loading as expected (Fig. 12*A*).

To determine which cells loaded with the dye in a CO_2-dependent manner, the slices containing the VMS were loaded with FITC, and the cellular localization of this dye was compared to that of conventional glial (GFAP) and neuronal (MAP2) markers. We found that increased P_{CO_2} allowed FITC entry into both the leptomeninges and the marginal glial layer (Fig. 12*B*–*E*). Interestingly the FITC loading often followed the tracks of penetrating blood vessels, reminiscent of the localization of Cx26 (Fig. 12*B*–*E* compare with Figs 10 and 11). FITC loading was colocalized with GFAP (Fig. 12*B* and *C*), but not with MAP2 (Fig. 12*D*). FITC labelling also colocalized with Cx26 immunoreactivity at the surface (glia limitans) and around penetrating blood vessels (Fig. 12*E*).

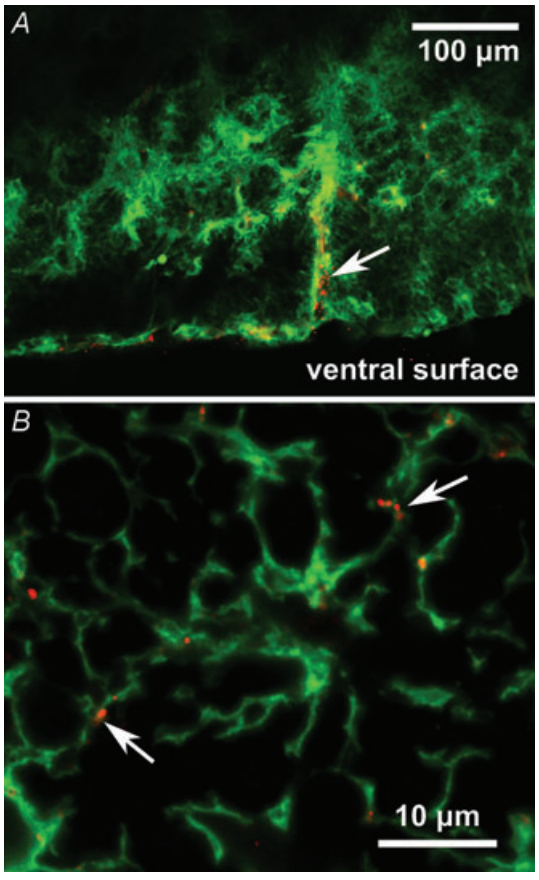

Figure 11. Immunocytochemical localization of Cx26 on astrocytes
A, Cx26-positive puncta (red) on astrocytes (green) located near the ventral surface (glia limitans) and ensheathing penetrating blood vessels (white arrow). *B*, at higher resolution Cx26 positive puncta can be seen (in a different tissue section) to be associated with astrocytic processes (white arrows). Tissue from rat.

Connexin hemichannel-mediated ATP release at the VMS contributes to the adaptive respiratory response to hypercapnia

The agents that we found to reduce CO_2-dependent ATP release *in vitro* (Co^{2+}, NPPB and proadifen, cf. Ripps *et al.* 2004; Zhao, 2005) are capable of partial but substantial block of Cx26 hemichannels. To explore whether there is a causal link between Cx26 hemichannel gating and the adaptive changes in breathing we used these compounds *in vivo*, and made recordings of the central respiratory drive (phrenic nerve discharge) and ATP release from the VMS in anaesthetized and artificially ventilated rats. Application of either NPPB or proadifen to the VMS had no effect on resting phrenic nerve discharge ($P > 0.1$) but greatly diminished CO_2-evoked ATP release and significantly reduced the resultant increases in respiratory activity (Fig. 13*A*–*C*). The degree of reduction in the CO_2-induced respiratory response following inhibition of hemichannel activity at the VMS was quantitatively similar to that previously reported for the action of ATP receptor antagonists applied to the VMS (Gourine *et al.* 2005*a*) and reflects the contribution of the VMS chemosensitive sites to the overall ventilatory response to CO_2 (Nattie, 2001).

Pharmacological studies of the roles of gap junction hemichannels have been hampered by a lack of highly selective agents to block these channels. It is possible therefore that the effects of NPPB and proadifen on the CO_2-evoked respiratory response, which have multiple targets, could have resulted from non-specific depression of respiratory network activity. As a control, we examined the effect of these agents on the respiratory responses to hypoxia in a similar rat preparation. Although responses to hypoxia depend on peripheral inputs from the carotid body, we have previously shown that there is a central component mediated by ATP release in the medulla oblongata (Gourine *et al.* 2005*b*). A brief period of hypoxia greatly enhances inspiratory activity (Fig. 14). Neither proadifen nor NPPB when applied to the VMS either separately or in combination had any effect on the resultant respiratory response (Fig. 14). Thus, these agents, at the concentrations used, neither induce a

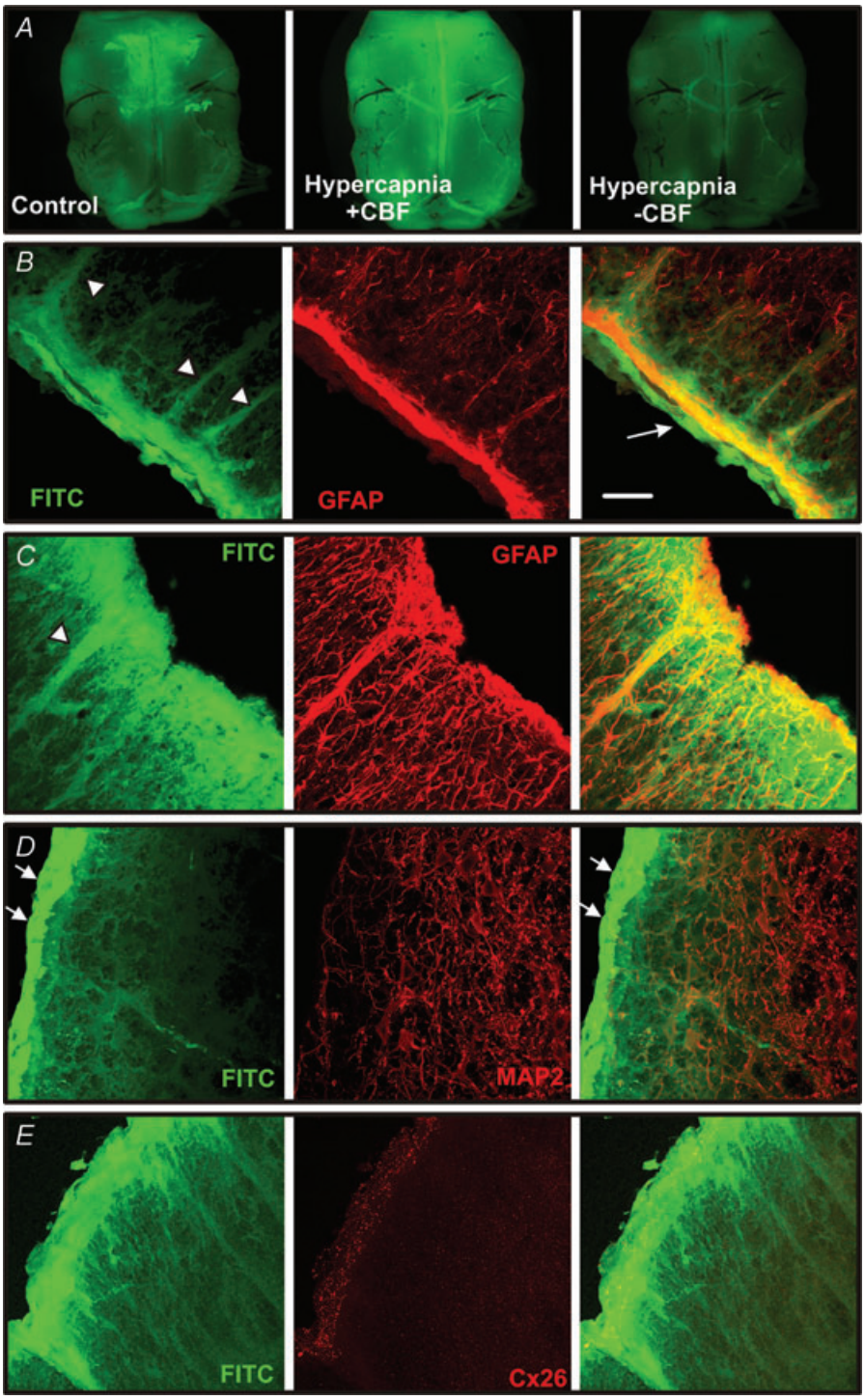

Figure 12. CO_2-dependent dye loading of the leptomeninges and astrocytes at the ventral medullary surface

A, whole mount images of a ventral medullary slice showing baseline loading following exposure to carboxyfluorescein (CBF) in control aCSF, greatly enhanced loading when exposed to CBF during hypercapnia (P_{CO_2} 60 mmHg) and diminished loading when P_{CO_2} was increased in the absence of CBF to flush out the previously loaded CBF. *B–E*, transverse sections showing FITC loading into the pia mater (arrow), the glia limitans and along the tracks of penetrating blood vessels (arrowheads). Note how the FITC colocalizes with GFAP staining suggesting that astrocytes are CO_2 sensitive (*B* and *C*). However, neurons stained with MAP2 do not dye load with FITC. The bright strip of FITC loaded tissue (white arrows) is the leptomeningeal layer. *D* and *E*, Cx26 immunostaining is located in the glia limitans where a high degree of CO_2-dependent dye loading occurs. Scale bar, 40 μm. All tissue from rat.

non-specific depression of respiratory network nor interfere with the operation of the reflex pathway responsible for increases in breathing following activation of the peripheral chemoreceptors. Together, our *in vivo* data strongly suggest that ATP released via Cx26 hemichannels contribute to the adaptive increases in ventilation in response to an increase in the levels of inspired CO_2.

Discussion

In this study we have replicated in an *in vitro* slice preparation of the ventral medulla containing the VMS of young adult rats an important central chemosensory transduction event – CO_2-dependent ATP release (Gourine *et al.* 2005*a*). This has allowed the detailed investigation of the facets of the chemosensory stimulus necessary for triggering ATP release, and the mechanisms by which ATP is released during hypercapnia.

Nature of the chemosensory stimulus which evokes ATP release from the VMS

As CO_2 and H_2O on are in equilibrium with H^+, HCO_3^-, fluctuations in CO_2 levels could in principle be detected either via a change in P_{CO_2} directly, extracellular or intracellular acidification, or via a change in [HCO_3^-]. There is evidence that small changes in extracellular pH trigger ATP release from the VMS (Gourine *et al.* 2010). The data presented here indicate that an increase in P_{CO_2} alone is also a sufficient stimulus to evoke release of ATP – the latter was observed in response to rising P_{CO_2} delivered at different constant levels of extracellular pH.

The case for intracellular HCO_3^- as the effective stimulus for triggering ATP release is weakened by the fact that acetazolamide, a membrane permeant inhibitor of carbonic anhydrase (Buckler *et al.* 1991), which catalyses the formation of H_2CO_3 and ultimately HCO_3^- and H^+, had no effect on either the amplitude or speed of CO_2 evoked ATP release. Furthermore acetazolamide had no effect on the resting level of ATP. Nevertheless all of the chemosensory stimulation protocols that we used did involve parallel changes in extracellular HCO_3^- (to control extracellular pH) and we cannot completely exclude the possibility that ATP release was triggered in part by changes in extracellular HCO_3^-. However, this is unlikely as in the accompanying paper we demonstrate that an increase in P_{CO_2} at constant HCO_3^- still gates open Cx26 hemichannels (Huckstepp *et al.* 2010).

To what extent could changes in intracellular pH represent the effective stimulus? Two agents that can directly alter intracellular pH, NH_4Cl and propionate, had no effect on the extracellular concentration of ATP at the VMS. NH_4Cl will initially cause intracellular

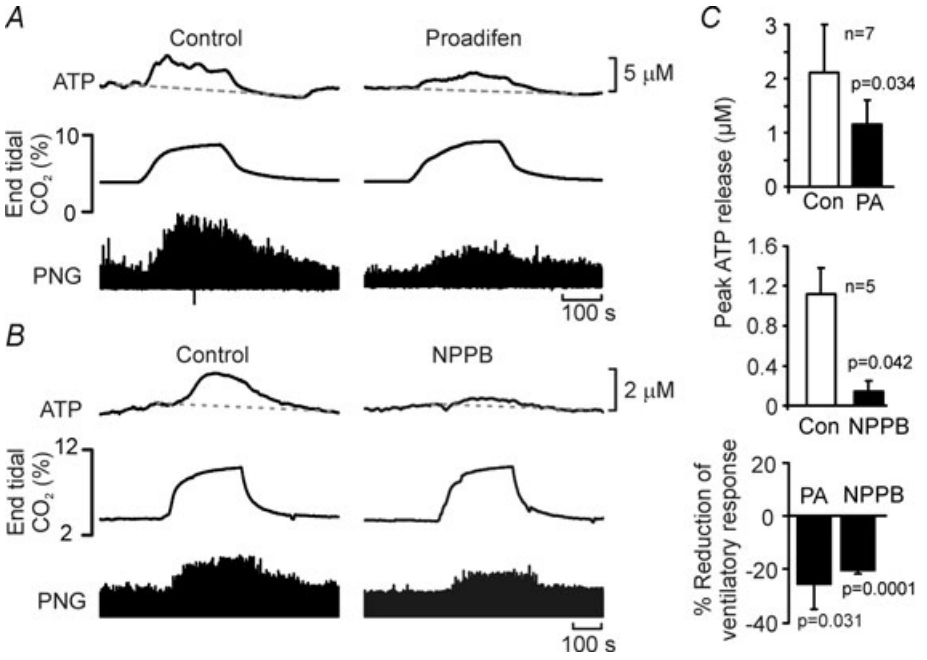

Figure 13. Hemichannel blockers reduce CO_2-evoked ATP release *in vivo* and diminish the adaptive respiratory response to CO_2

A and *B*, the effects of proadifen (PA, 200 μM) and NPPB (200 μM) on ATP release and the adaptive respiratory response to CO_2 in anaesthetized and artificially ventilated rats (PNG – integrated phrenic neurogram). Both ATP release and the respiratory responses were reduced. *C*, summary data showing the concentrations of CO_2-evoked ATP release and reduction of the respiratory response in the absence and presence of proadifen and NPPB on the ventral surface of the medulla oblongata (comparisons paired sample *t* tests).

alkalinization, but this is followed by acidification in many cells (Ritucci *et al.* 1998). The concentration of propionate that we used was rather low to avoid confounding signals on the biosensor, but these levels have been shown to reduce intracellular pH by as much as 0.3 units (Shono *et al.* 2010). That acetazolamide had no effect on the dynamics of ATP release also weakens the case for a change in intracellular pH, as carbonic anhydrase is needed to mediate the rapid intracellular acidification that accompanies an increase in P_{CO_2} – thus we would have expected ATP release to be slowed in the presence of acetazolamide if this were the case. Although we cannot absolutely eliminate intracellular pH as the effective signal, as we did not measure this variable directly, in the accompanying paper we demonstrate under conditions of constant pH that CO_2 modulates Cx26 hemichannel opening in inside-out and outside-out excised membrane patches (Huckstepp *et al.* 2010). This further weakens the case for intracellular pH as the chemosensory stimulus for inducing the release of ATP.

A further issue that we addressed here is whether a CO_2/HCO_3-sensitive adenylate cyclase might be involved and cause ATP release through cAMP-dependent signalling. However blockade of adenylate cyclases with SQ22536 had no effect on CO_2-evoked ATP release. We therefore propose that CO_2 itself is one of the main stimuli, which evokes the ATP release from the VMS during hypercapnia.

Gap junction hemichannels mediate ATP release in response to CO_2

CO_2-dependent ATP release appears to occur via the opening of a gap junction hemichannel. Several lines of evidence support this. ATP release is independent of extracellular Ca^{2+}, and removal of extracellular Ca^{2+} itself, a condition that triggers opening of gap junction hemichannels, causes ATP release from the VMS. This manipulation presumably increases the opening of all connexin hemichannel types present in the ventral medulla, giving rise to the large level of ATP release observed. That a CO_2 stimulus under these conditions can still cause enhanced ATP release is presumably due to its acting specifically on Cx26 and via a mechanism independent of the divalent modulation of the hemichannel gating, such that it could cause even greater channel opening and hence additional ATP release.

Both the CO_2-evoked ATP release and the zero Ca^{2+} evoked release are substantially inhibited by the application of several compounds that can block hemichannels. None of these compounds are specific for hemichannels; nevertheless they all have different off target

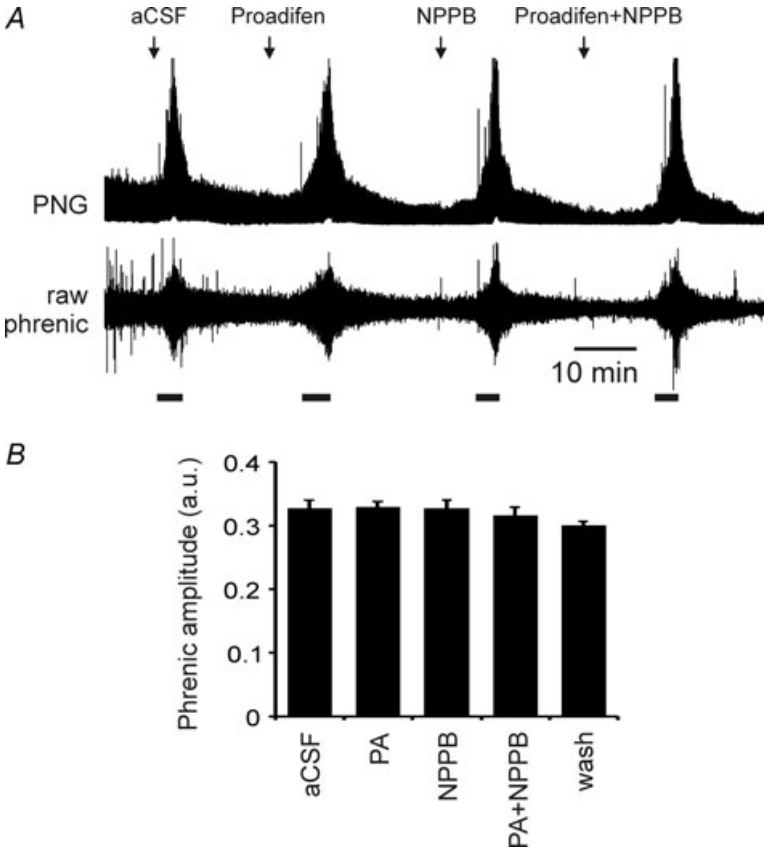

Figure 14. Hemichannel blockers do not affect the respiratory response to systemic hypoxia *in vivo*
A, neither proadifen (PA, 200 μM) nor NPPB (200 μM) altered the increases in phrenic nerve activity (PNG – integrated phrenic neurogram) evoked by 5 min of 10% hypoxia (thick bars) in an anaesthetized and ventilated rat. The combination of both agents had no effect either. ($n = 4$ rats.) *B*, changes in phrenic nerve amplitude in response to hypoxia under control conditions and in the presence of the hemichannel blockers.

effects – that they all block both forms of ATP release strongly suggests a role for gap junction hemichannels.

The role of hemichannels in mediating CO_2-evoked ATP release is further strengthened by the results of the dye-loading experiments, which demonstrate opening of a sufficiently large channel in response to an increase in P_{CO_2} to allow the influx of carboxyfluorescein or FITC (molecular weights of ∼380). The dye loads into the leptomeninges and subpial astrocytes as well as astrocytes that ensheath the penetrating blood vessels. These two lines of evidence strongly suggest that hemichannels gate open to allow the efflux of ATP during elevated P_{CO_2}.

Interestingly there is a high basal tone of ATP at the VMS. This basal tone also appears to arise from release via hemichannels – it was greatly reduced by agents that act on these channels. Furthermore we observed a background level of dye loading in the slices at normal physiological levels of P_{CO_2}. This is again consistent with the idea of a resting level of hemichannel gating that is sufficient to allow a low level of tonic efflux of ATP (and hence dye loading). That such a large resting tone is measurable suggests a continual source of ATP release.

The identity of the gap junction hemichannel mediating CO_2-evoked ATP release from the VMS

There are two major gene families of gap junction proteins capable of forming hemichannels – the pannexins and connexins. Our pharmacological data eliminate pannexin-1 as a mediator of ATP release. CO_2-dependent ATP release is unaffected by the presence of blockers selective for this channel (low doses of carbenoxolone and probenecid). All of the other agents that we used to block CO_2-dependent ATP release act on Cx26 hemichannels and indeed Cx26 is our favoured candidate to mediate CO_2-dependent ATP release.

Although Cx26 is not the most abundant connexin in the ventral medulla, of the connexins present in the medulla oblongata, only Cx26 has a selective distribution near the VMS as determined by quantitative PCR, immunocytochemistry and a knock-in reporter. It is present in the leptomeninges, the glia limitans and cells close to penetrating blood vessels. In addition there was great similarity between the distribution of Cx26-expressing cells and the cell types and pattern of CO_2-dependent dye loading. Indeed we find that Cx26 is expressed on the surface of the cells that dye load in response to increased P_{CO_2}. Our finding, reported in the accompanying paper (Huckstepp *et al.* 2010), that Cx26 is directly sensitive to changes in P_{CO_2} in the physiological range, leaves little doubt that this connexin hemichannel contributes to CO_2-dependent ATP release.

Physiological significance

Our pharmacological data obtained with the use of a range of hemichannel blockers support a causal link between gating of Cx26 hemichannel at the VMS and the adaptive respiratory responses to changes in inspired CO_2. We utilized two different blockers (NPPB and proadifen), both known to inhibit Cx26. As a control for non-specific actions of these agents on the respiratory network or reflex pathways from the peripheral chemoreceptors, we demonstrated that neither NPPB nor proadifen altered hypoxia-evoked increases in central respiratory drive. However, since deletion of Cx26 is embryonic lethal (Gabriel *et al.* 1998), and Cx26 is involved in the early development of brain (Elias *et al.* 2007) and other tissues, genetic dissection of the role of Cx26 in central chemosensory transduction will await the development of tissue specific inducible knock-out animal models.

We have demonstrated here that hypercapnia-evoked ATP release at the VMS depends in part directly on changes in P_{CO_2}. The CO_2-dependent release of ATP is modulated by extracellular pH. Acidification causes a rightward shift in the relationship between ATP release and CO_2, while alkalinization shifts the relation leftwards and allows smaller absolute levels of P_{CO_2} to evoke ATP release. This inhibitory effect of acidification on the CO_2-evoked release of ATP could potentially reduce its contribution to chemosensing depending on the extent of the accompanying pH change. However the critical factor is the pH at the vicinity of Cx26 and local buffering could conceivably limit the pH change around the glial cells and Cx26 compared to that of the bulk extracellular fluid.

Interestingly, at resting levels of P_{CO_2}, we found a high basal tone of ATP in the chemosensitive areas, supporting the hypothesis that ATP provides a continual excitatory drive to the respiratory network (Thomas *et al.* 1999). Fluctuations in P_{CO_2} above and below the normal physiological level respectively increase and decrease release of ATP from the VMS. Thus, this is a bidirectional control system, which has all the features required to contribute to modulation of the activity of the respiratory network and, therefore, ventilation in accord with prevailing CO_2 tension in the brain parenchyma.

In man mutations of Cx26 (also known as GJB2) are some of the commonest causes of non-syndromal sensorineural hearing loss (Rabionet *et al.* 2000; Petersen & Willems 2006). Yet altered ventilatory drive has not been reported in these patient cohorts. There are several possible reasons for this. Firstly, the CO_2-sensitive feature of Cx26 and its role in the supporting cells of the cochlea may involve different and independent aspects of the molecule. Thus a mutation that affects one role may not affect the other. Secondly, for those mutations that prevent expression of functional protein (e.g. premature stop codons, Kelley *et al.* 1998), compensatory changes

in the expression of other CO_2-sensitive connexins such as Cx30 and Cx32 (Huckstepp *et al*. 2010) may diminish any breathing phenotype. Thirdly, if the nature of the respiratory deficit were to be highly variable (taking a known defect of central chemoreception – congenital central hypoventilation syndrome – as a precedent), it may simply have gone unremarked in the potentially small proportion of profoundly deaf patients where this could arise. Our work suggests that it is worth investigating whether altered ventilatory drive can be observed in a cohort of genotyped Cx26-deficient patients.

Cx26 is expressed in the leptomeninges and glia limitans but not in neurons, and thus both cell types are potentially capable of releasing ATP in a CO_2-dependent manner. This suggests that the leptomeninges and glia limitans may play a much more important role in the central respiratory chemosensory reflex than has been hitherto appreciated. As Cx26 is expressed in cells that line penetrating blood vessels (arterioles and capillaries), it might conceivably play a role in CO_2-dependent vasodilatation and thus contribute to the regulation of cerebral blood flow during the chemosensory reflex, which will alter the relationship between arterial P_{CO_2}, and pH and those of the brain parenchyma.

Parallel pathways of central respiratory chemosensory transduction

The possibility that CO_2 levels are detected via changes in extracellular pH is well documented (Winterstein, 1949; Loeschcke, 1982). However several studies have revealed that changes in extracellular pH unaccompanied by an increase in P_{CO_2} evoke much weaker adaptive changes in respiration compared to similar levels of acidification driven by an elevation of P_{CO_2} ('metabolic' and 'respiratory' acidosis, respectively; Eldridge *et al.* 1985; Shams, 1985; Putnam *et al.* 2004). Some have suggested that intracellular acidification is an important aspect of central chemosensitivity (Putnam *et al.* 2004). While our data do not support intracellular pH as a factor for triggering ATP release during hypercapnia, they do strongly suggest that ATP release depends on the prevailing P_{CO_2} directly. This identifies a parallel CO_2-sensitive pathway that could act additively with the pH sensing pathway and thus account for the different magnitudes of cellular and systemic respiratory responses evoked by metabolic *versus* respiratory acidosis.

CO_2 chemoreception seems to involve several brainstem nuclei including the medullary raphé, the RTN and the locus coeruleus (Nattie & Li, 2009). Our observation that only about 20% of the response to hypercapnia is blocked by inhibitors of hemichannel mediated ATP release when applied to the VMS is consistent with this hypothesis of multiple sites of chemosensitivity. The Cx26-mediated mechanism of CO_2-evoked ATP release may also contribute to chemosensing in several of these other nuclei. We note that populations of neurons proposed as central respiratory pH chemosensors, including the RTN, medullary raphé and locus coeruleus, are all sensitive to ATP (Nieber *et al.* 1997; Yao *et al.* 2000; Mulkey *et al.* 2006; Cao & Song, 2007). These neural populations could therefore represent the distributed sites of convergence for the neuronally mediated pH sensing and the ATP-mediated CO_2 sensing components of central respiratory chemosensitivity. We have demonstrated here that the ATP released during hypercapnia can diffuse at least 400 μm deep into the tissue, suggesting that it should be able to activate the chemosensitive neurons of the RTN and medullary raphé. Indeed, in contrast to earlier observations by Mulkey *et al.* (2006), recent evidence in organotypic slices demonstrates that both pH-evoked depolarizations and Ca^{2+} responses of Phox2b-expressing RTN neurones are almost entirely mediated by prior release of ATP (Gourine *et al.* 2010). Equally it remains to be determined whether this mechanism also operates at the dorsal surface of the brainstem where glial-derived ATP released via Cx26 could excite locus coeruleus neurons.

The RTN neurons express the transcription factor *Phox2b* (Stornetta *et al.* 2006). Mutations of this gene are associated with central congenital hypoventilation syndrome (CCHS) in humans. Introduction of these mutations into mice or selective depletion of *Phox2b*-expressing RTN neurons can severely disrupt breathing and results in a complete loss of CO_2 sensitivity in the neonate (Dubreuil *et al.* 2008, 2009). The effect of these mutations on adult chemosensitivity has not been reported. In humans with CCHS, the symptoms often lessen with age (Shea, 1997; Chen & Keens, 2004). It is entirely possible that the role of *Phox2b*-expressing neurons is particularly important for chemoreception in the neonate but lessens with development as other chemosensory transduction mechanisms develop and other areas of the brainstem become important. Indeed in $Phox2b^{+/-}$ heterozygotes, impaired responses to hypercapnia evident at age P2 are largely normalized by P10 (Dauger *et al.* 2003). We propose that the CO_2-sensitive Cx26 hemichannel-mediated mechanism of ATP release may play an important role in parallel to the chemosensitivity mediated by specific populations of pH-sensitive neurons in central respiratory chemosensitivity in the adult.

References

Bradley SR, Pieribone VA, Wang W, Severson CA, Jacobs RA & Richerson GB (2002). Chemosensitive serotonergic neurons are closely associated with large medullary arteries. *Nat Neurosci* **5**, 401–402.

Bruzzone R, Barbe MT, Jakob NJ & Monyer H (2005). Pharmacological properties of homomeric and heteromeric pannexin hemichannels expressed in *Xenopus* oocytes. *J Neurochem* **92**, 1033–1043.

Buckler KJ, Vaughan-Jones RD, Peers C & Nye PC (1991). Intracellular pH and its regulation in isolated type I carotid body cells of the neonatal rat. *J Physiol* **436**, 107–129.

Cao Y & Song G (2007). Purinergic modulation of respiration via medullary raphe nuclei in rats. *Respir Physiol Neurobiol* **155**, 114–120.

Chen ML & Keens TG (2004). Congenital central hypoventilation syndrome: not just another rare disorder. *Paediatr Respir Rev* **5**, 182–189.

Corcoran AE, Hodges MR, Wu Y, Wang W, Wylie CJ, Deneris ES & Richerson GB (2009). Medullary serotonin neurons and central CO_2 chemoreception. *Respir Physiol Neurobiol* **168**, 49–58.

Dauger S, Pattyn A, Lofaso F, Gaultier C, Goridis C, Gallego J & Brunet JF (2003). Phox2b controls the development of peripheral chemoreceptors and afferent visceral pathways. *Development* **130**, 6635–6642.

Drummond GB (2009). Reporting ethical matters in *The Journal of Physiology*: standards and advice. *J Physiol* **587**, 713–719.

Dubreuil V, Ramanantsoa N, Trochet D, Vaubourg V, Amiel J, Gallego J, Brunet JF & Goridis C (2008). A human mutation in Phox2b causes lack of CO_2 chemosensitivity, fatal central apnea, and specific loss of parafacial neurons. *Proc Natl Acad Sci U S A* **105**, 1067–1072.

Dubreuil V, Thoby-Brisson M, Rallu M, Persson K, Pattyn A, Birchmeier C, Brunet JF, Fortin G & Goridis C (2009). Defective respiratory rhythmogenesis and loss of central chemosensitivity in Phox2b mutants targeting retrotrapezoid nucleus neurons. *J Neurosci* **29**, 14836–14846.

Eldridge FL, Kiley JP & Millhorn DE (1985). Respiratory responses to medullary hydrogen ion changes in cats: different effects of respiratory and metabolic acidoses. *J Physiol* **358**, 285–297.

Elias LA, Wang DD & Kriegstein AR (2007). Gap junction adhesion is necessary for radial migration in the neocortex. *Nature* **448**, 901–907.

Feldman JL, Mitchell GS & Nattie EE (2003). Breathing: rhythmicity, plasticity, chemosensitivity. *Annu Rev Neurosci* **26**, 239–266.

Filippov MA, Hormuzdi SG, Fuchs EC & Monyer H (2003). A reporter allele for investigating connexin 26 gene expression in the mouse brain. *Eur J Neurosci* **18**, 3183–3192.

Filosa JA, Dean JB & Putnam RW (2002). Role of intracellular and extracellular pH in the chemosensitive response of rat locus coeruleus neurones. *J Physiol* **541**, 493–509.

Gabriel HD, Jung D, Butzler C, Temme A, Traub O, Winterhager E & Willecke K (1998). Transplacental uptake of glucose is decreased in embryonic lethal connexin26-deficient mice. *J Cell Biol* **140**, 1453–1461.

Gourine AV, Atkinson L, Deuchars J & Spyer KM (2003). Purinergic signalling in the medullary mechanisms of respiratory control in the rat: respiratory neurones express the P2X2 receptor subunit. *J Physiol* **552**, 197–211.

Gourine AV, Llaudet E, Dale N & Spyer KM (2005*a*). ATP is a mediator of chemosensory transduction in the central nervous system. *Nature* **436**, 108–111.

Gourine AV, Llaudet E, Dale N & Spyer KM (2005*b*). Release of ATP in the ventral medulla during hypoxia in rats: Role in hypoxic ventilatory response. *J Neurosci* **25**, 1211–1218.

Gourine AV, Dale N, Korsak A, Llaudet E, Tian F, Huckstepp R & Spyer KM (2008). Release of ATP and glutamate in the nucleus tractus solitarii mediate pulmonary stretch receptor (Breuer-Hering) reflex pathway. *J Physiol* **586**, 3963–3978.

Gourine AV, Kasymov V, Marina N, Tang F, Figueiredo MF, Lane S, Teschemacher AG, Spyer KM, Deisseroth K, Kasparov S (2010) Astrocytes control breathing through pH-dependent release of ATP. *Science* **329**, 571–575.

Grocott MP, Martin DS, Levett DZ, McMorrow R, Windsor J & Montgomery HE (2009). Arterial blood gases and oxygen content in climbers on Mount Everest. *N Engl J Med* **360**, 140–149.

Guyenet PG (2008). The 2008 Carl Ludwig Lecture: retrotrapezoid nucleus, CO_2 homeostasis, and breathing automaticity. *J Appl Physiol* **105**, 404–416.

Huckstepp RTR, Eason R, Sachdev A & Dale N (2010). CO_2-dependent opening of connexin 26 and related β connexins. *J Physiol* **588**, 3921–3931.

Kawai A, Ballantyne D, Muckenhoff K & Scheid P (1996). Chemosensitive medullary neurones in the brainstem–spinal cord preparation of the neonatal rat. *J Physiol* **492**, 277–292.

Kelley PM, Harris DJ, Comer BC, Askew JW, Fowler T, Smith SD & Kimberling WJ (1998). Novel mutations in the connexin 26 gene (GJB2) that cause autosomal recessive (DFNB1) hearing loss. *Am J Hum Genet* **62**, 792–799.

Llaudet E, Hatz S, Droniou M & Dale N (2005). Microelectrode biosensor for real-time measurement of ATP in biological tissue. *Anal Chem* **77**, 3267–3273.

Loeschcke HH (1982). Central chemosensitivity and the reaction theory. *J Physiol* **332**, 1–24.

Mercier F & Hatton GI (2001). Connexin 26 and basic fibroblast growth factor are expressed primarily in the subpial and subependymal layers in adult brain parenchyma: roles in stem cell proliferation and morphological plasticity? *J Comp Neurol* **431**, 88–104.

Mittag TW, Guo WB & Kobayashi K (1993). Bicarbonate-activated adenylyl cyclase in fluid-transporting tissues. *Am J Physiol Renal Physiol* **264**, F1060–1064.

Mulkey DK, Stornetta RL, Weston MC, Simmons JR, Parker A, Bayliss DA & Guyenet PG (2004). Respiratory control by ventral surface chemoreceptor neurons in rats. *Nat Neurosci* **7**, 1360–1369.

Mulkey DK, Mistry AM, Guyenet PG & Bayliss DA (2006). Purinergic P2 receptors modulate excitability but do not mediate pH sensitivity of RTN respiratory chemoreceptors. *J Neurosci* **26**, 7230–7233.

Mulkey DK, Talley EM, Stornetta RL, Siegel AR, West GH, Chen X, Sen N, Mistry AM, Guyenet PG & Bayliss DA (2007). TASK channels determine pH sensitivity in select respiratory neurons but do not contribute to central respiratory chemosensitivity. *J Neurosci* **27**, 14049–14058.

Muller DJ, Hand GM, Engel A & Sosinsky GE (2002). Conformational changes in surface structures of isolated connexin 26 gap junctions. *EMBO J* **21**, 3598–3607.

Nagy JI, Li X, Rempel J, Stelmack G, Patel D, Staines WA, Yasumura T & Rash JE (2001). Connexin26 in adult rodent central nervous system: demonstration at astrocytic gap junctions and colocalization with connexin30 and connexin43. *J Comp Neurol* **441**, 302–323.

Nattie EE & Li A (1996). Central chemoreception in the region of the ventral respiratory group in the rat. *J Appl Physiol* **81**, 1987–1995.

Nattie EE (2001). Central chemosensitivity, sleep, and wakefulness. *Respir Physiol* **129**, 257–268.

Nattie EE & Li A (2008). Multiple central chemoreceptor sites: cell types and function in vivo. *Adv Exp Med Biol* **605**, 343–347.

Nattie E & Li A (2009). Central chemoreception is a complex system function that involves multiple brain stem sites. *J Appl Physiol* **106**, 1464–1466.

Nieber K, Poelchen W & Illes P (1997). Role of ATP in fast excitatory synaptic potentials in locus coeruleus neurones of the rat. *Br J Pharmacol* **122**, 423–430.

Pearson RA, Dale N, Llaudet E & Mobbs P (2005). ATP released via gap junction hemichannels from the pigment epithelium regulates neural retinal progenitor proliferation. *Neuron* **46**, 731–744.

Petersen MB & Willems PJ (2006). Non-syndromic, autosomal-recessive deafness. *Clin Genet* **69**, 371–392.

Putnam RW, Filosa JA & Ritucci NA (2004). Cellular mechanisms involved in CO_2 and acid signaling in chemosensitive neurons. *Am J Physiol Cell Physiol* **287**, C1493–1526.

Putnam RW, Conrad SC, Gdovin MJ, Erlichman JS & Leiter JC (2005). Neonatal maturation of the hypercapnic ventilatory response and central neural CO_2 chemosensitivity. *Respir Physiol Neurobiol* **149**, 165–179.

Rabionet R, Gasparini P & Estivill X (2000). Molecular genetics of hearing impairment due to mutations in gap junction genes encoding beta connexins. *Hum Mutat* **16**, 190–202.

Raven JA (2006). Sensing inorganic carbon: CO_2 and HCO_3. *Biochem J* **396**, e5–7.

Richerson GB (2004). Serotonergic neurons as carbon dioxide sensors that maintain pH homeostasis. *Nat Rev Neurosci* **5**, 449–461.

Ritucci NA, Chambers-Kersh L, Dean JB & Putnam RW (1998). Intracellular pH regulation in neurons from chemosensitive and nonchemosensitive areas of the medulla. *Am J Physiol Regul Integr Comp Physiol* **275**, R1152–1163.

Ritucci NA, Erlichman JS, Leiter JC & Putnam RW (2005). Response of membrane potential and intracellular pH to hypercapnia in neurons and astrocytes from rat retrotrapezoid nucleus. *Am J Physiol Regul Integr Comp Physiol* **289**, R851–861.

Ripps H, Qian HH & Zakevicius J (2004). Properties of connexin26 hemichannels expressed in *Xenopus* oocytes. *Cell Mol Neurobiol* **24**, 647–665.

Severson CA, Wang W, Pieribone VA, Dohle CI & Richerson GB (2003). Midbrain serotonergic neurons are central pH chemoreceptors. *Nat Neurosci* **6**, 1139–1140.

Shams H (1985). Differential effects of CO_2 and H^+ as central stimuli of respiration in the cat. *J Appl Physiol* **58**, 357–364.

Shea SA (1997). Life without ventilatory chemosensitivity. *Respir Physiol* **110**, 199–210.

Shono Y, Kamouchi M, Kitazono T, Kuroda J, Nakamura K, Hagiwara N, Ooboshi H, Ibayashi S & Iida M (2010). Change in intracellular pH causes the toxic Ca^{2+} entry via NCX1 in neuron- and glia-derived cells. *Cell Mol Neurobiol* **30**, 453–460.

Silverman W, Locovei S & Dahl GP (2008). Probenecid, a gout remedy, inhibits pannexin 1 channels. *Am J Physiol Cell Physiol* **295**, C761–767.

Solomon IC, Halat TJ, El-Maghrabi MR & O'Neal MH 3rd (2001). Localization of connexin26 and connexin32 in putative CO_2-chemosensitive brainstem regions in rat. *Respir Physiol* **129**, 101–121.

Stornetta RL, Moreira TS, Takakura AC, Kang BJ, Chang DA, West GH, Brunet JF, Mulkey DK, Bayliss DA & Guyenet PG (2006). Expression of Phox2b by brainstem neurons involved in chemosensory integration in the adult rat. *J Neurosci* **26**, 10305–10314.

Summers BA, Overholt JL & Prabhakar NR (2002). CO_2 and pH independently modulate L-type Ca^{2+} current in rabbit carotid body glomus cells. *J Neurophysiol* **88**, 604–612.

Thomas T, Ralevic V, Gadd CA & Spyer KM (1999). Central CO_2 chemoreception: a mechanism involving P2 purinoceptors localized in the ventrolateral medulla of the anaesthetized rat. *J Physiol* **517**, 899–905.

Trapp S, Aller MI, Wisden W & Gourine AV (2008). A role for TASK-1 (KCNK3) channels in the chemosensory control of breathing. *J Neurosci* **28**, 8844–8850.

Wilson MH, Newman S & Imray CH (2009). The cerebral effects of ascent to high altitudes. *Lancet Neurol* **8**, 175–191.

Winterstein H (1949). The reaction theory of respiratory regulation. *Experientia* **5**, 221–226.

Wu J, Xu H, Shen W & Jiang C (2004). Expression and coexpression of CO_2-sensitive Kir channels in brainstem neurons of rats. *J Membr Biol* **197**, 179–191.

Yamamoto Y, Ishikawa R, Omoe K, Yoshikawa N, Yamaguchi-Yamada M & Taniguchi K (2008). Immunohistochemical distribution of inwardly rectifying K^+ channels in the medulla oblongata of the rat. *J Vet Med Sci* **70**, 265–271.

Yao ST, Barden JA, Finkelstein DI, Bennett MR & Lawrence AJ (2000). Comparative study on the distribution patterns of $P2X_1$-$P2X_6$ receptor immunoreactivity in the brainstem of the rat and the common marmoset (*Callithrix jacchus*): association with catecholamine cell groups. *J Comp Neurol* **427**, 485–507.

Zhao HB (2005). Connexin26 is responsible for anionic molecule permeability in the cochlea for intercellular signalling and metabolic communications. *Eur J Neurosci* **21**, 1859–1868.

Author contributions

R.T.R.H. and R.idB. performed the *in vitro* slice experiments and analysed the data. R.E. assisted by R.T.R.H. performed and analysed the immunocytochemistry and QPCR, K.M.S. advised on *in vivo* experiments, A.V.G. helped to design the

study, and performed the *in vivo* work assisted by R.T.R.H., and N.M. performed Cx26 immunolabelling. N.D. (Bonn) and K.W. generated the $Cx26^{+/lacZ}$ mice and provided the tissue. N.D. (Warwick) conceived the study, directed the work and wrote the manuscript. All authors read and commented on the manuscript. All *in vitro* experiments were performed at Warwick, the *in vivo* experiments were performed at University College London.

Acknowledgements

We thank the MRC (N.D.), BBSRC (N.D.) and Wellcome Trust (A.V.G.) for generous support. A.V.G. is a Wellcome Trust Senior Research Fellow. The generation and characterization of $Cx26^{+/LacZ}$ mice in the Bonn laboratory has been supported by the German Research Association (SFB 645, B2) and the Juergen Manchot Foundation.